01 Jan 2007

Adaptive Power Control Protocol with Hardware Implementation for Wireless Sensor and RFID Reader Networks

Kainan Cha

Jagannathan Sarangapani
Missouri University of Science and Technology, sarangap@mst.edu

David Pommerenke
Missouri University of Science and Technology, davidjp@mst.edu

Recommended Citation

K. Cha et al., "Adaptive Power Control Protocol with Hardware Implementation for Wireless Sensor and RFID Reader Networks," *IEEE Systems Journal*, Institute of Electrical and Electronics Engineers (IEEE), Jan 2007.
The definitive version is available at https://doi.org/10.1109/JSYST.2007.907682

Adaptive Power Control Protocol With Hardware Implementation for Wireless Sensor and RFID Reader Networks

Kainan Cha, S. Jagannathan, *Senior Member, IEEE*, and David Pommerenke

***Abstract*—The development and deployment of radio frequency identification (RFID) systems render a novel distributed sensor network which enhances visibility into manufacturing processes. In RFID systems, the detection range and read rates will suffer from interference among high-power reading devices. This problem grows severely and degrades system performance in dense RFID networks. Consequently, medium access protocols (MAC) protocols are needed for such networks to assess and provide access to the channel so that tags can be read accurately. In this paper, we investigate a suite of feasible power control schemes to ensure overall coverage area of the system while maintaining a desired read rate. The power control scheme and MAC protocol dynamically adjust the RFID reader power output in response to the interference level seen during tag reading and acceptable signal-to-noise ratio (SNR). We present novel distributed adaptive power control (DAPC) as a possible solution. A suitable back off scheme is also added with DAPC to improve coverage. A generic UHF wireless testbed is built using UMR/SLU GEN4-SSN for implementing the protocol. Both the methodology and hardware implementation of the schemes are presented, compared, and discussed. The results of hardware implementation illustrate that the protocol performs satisfactorily as expected.**

***Index Terms*—Coverage optimization, distributed power control, frequency interference, radio frequency identification (RFID), reader collision, sensor networks.**

I. Introduction

THE ADVENT of radio frequency identification (RFID) technology has brought with it increased visibility into manufacturing process and industry. From supply chain logistics to enhanced shop floor control, this technology presents many opportunities for process improvement or reengineering. The underlying principle of RFID technology is to obtain information from tags by using readers through radio frequency (RF) links. Low cost and small RFID tags can be viewed as a type of sensor since they provide identity and location information. A cluster of readers working together can monitor the flow of tags and obtain information about the distributed process or the supply chain. Consequently, the RFID network can be viewed as a distributed sensor network. Other sensors with radio links can be included as part of the RFID network as observed in a real word scenario. The RFID technology basics and current standards can be found in [1].

In passive RFID systems, tags harvest energy from the carrier signal which is obtained from the reader to power internal circuits. Therefore, passive tags do not initiate any communication but they only decode modulated command signals from the readers and respond accordingly through backscatter communication [1]. The nature of RF backscatter [2] requires high-power output at the reader and theoretically higher output power offers farther detection range with a desirable bit error rate (BER). For 915-MHz ISM bands, the output power is limited to 1 W according to [3]. When multiple readers are deployed in a working environment, signals from one reader may reach others and cause interference, for instance, in a dock door industrial environment. This interference problem was explained in [4] as the *Reader Collision*.

The work in [4] suggested that RFID *frequency interference* occurs when a signal transmitted from one reader reaches another and jams its ongoing communication with tags in range. Studies also show that, interrogation zones among readers need not overlap for *frequency interference* to occur, the reason being power radiated from one reader needs to be at the level of tag backscatter signal (μW) [4] to cause interference when reaching others. For a desired coverage area, readers must be placed relatively close to one another forming a dense reader network. Consequently, *frequency interference* normally occurs which results in limited read range, inaccurate reads, and long reading intervals. Placement of readers to minimize the interference and maximize the read range is an open problem.

To date, *frequency interference* has been described as "collision" as in a *yes* or *no* case where a reader in the same channel at a certain distance causes another reader not to read any of its tags in its range. In fact, higher interference only implies that the read range is reduced significantly but not to zero. This result is mathematically given in Section II. Previous attempts [5], [6] to solve this channel access problem are based on either spectral or temporal separation of readers. Colorwave [5] and "listen before talk" [7] implemented as per European Conference of Postal and Telecommunications Administration (CEPT) regulations [6] rely on time-based separation while frequency hopping spread spectrum (FHSS) implemented as per the FCC regulations [3] utilize multiple frequency channels. The former strategy is inefficient in terms of reader time and average read

Manuscript received August 30, 2007. This work was supported in part by the Center for Aerospace Manufacturing Technologies under the AFRL Grant, by the NSF STTR Award, and by the Intelligent Systems Center.

K. Cha is with Garmin International, Kansas City, KS 66062 USA.

S. Jagannathan and D. Pommerenke are with the Department of Electrical and Computer Engineering, University of Missouri–Rolla, Rolla 65409 USA (e-mail: sarangap@umr.edu).

Color versions of one or more of the figures in this paper are available online at http://ieeexplore.ieee.org.

Digital Object Identifier 10.1109/JSYST.2007.907682

range while the latter is not universally permitted by regulations. The proposed work is targeted for RFID networks to overcome these limitations.

In this paper, we propose a novel power control scheme which employs reader transmission power as the system control variable to achieve a desired read range and read rates. The degree of interference measured at each reader is used as a local feedback parameter to dynamically adjust its transmission power. With the same underlying concept, decentralized adaptive power control uses signal-to-noise ratio (SNR) to adapt power at discrete-time steps while probabilistic power control adapts the transmission power based on certain probability distribution. A Lyapunov-based approach is used to show the convergence of the proposed adaptive power control (DAPC) scheme. Simulation results demonstrate theoretical conclusions.

In terms of organization, the paper discusses the problem formulation in Section II. Then the decentralized power control algorithm is presented in Section III. Section IV details the simulation setup, whereas Section V presents hardware implementation including hardware and software architecture. In Section VI, results obtained from simulation and hardware implementation are discussed. Subsequently, the conclusions are presented.

II. Problem Formulation

The *frequency interference* problem needs to be fully understood before a solution can be evolved. In this section, we present analysis of this problem and assumptions made.

A. Mathematical Relations

In a backscatter communication system such as the case of a passive RFID system, SNR must meet a required threshold R_{required}, which can be expressed as

$$R_{\text{required}} = (E_b/N_0)/(W/D) \tag{1}$$

where E_b is the energy/bit of the received signal in watts, N_0 is the noise power in watts per hertz, D is the bit rate in bits per second, and W is the radio channel bandwidth in Hertz. For a known modulation method and bit-error rate (BER), E_b/N_0 can be calculated. Hence, R_{required} can be selected based on desired read rate and BER.

For any reader i, the following must hold for successful tag detection:

$$\frac{P_{bs}}{I_i} = R_i \geq R_{\text{required}} \tag{2}$$

where P_{bs} is the backscatter power from a tag, I_i is the interference at the tag backscatter frequency, and R_i is the SNR at a given reader "i."

In general, P_{bs} can be evaluated in terms of the reader transmission power P_i and tag distance r_{i-t}. Other variables such as reader and tag antenna gains, modulation indexing and wavelength, derived in [7], can be considered as constants and simplified in (3) as K_1. Then

$$P_{bs} = K_1 \cdot \frac{P_i}{r_{i-t}^{4q}} = g_{ii} \cdot P_i \tag{3}$$

where q is environment dependent variable considering path loss and g_{ii} represents the channel loss from reader i to tag and back. Communication channel between the reader and interrogated tag should be in relatively short range, for this reason Rayleigh fading and Shadowing effects are not considered for the reader-tag link. Channel uncertainties such as path loss can be considered as a part of g_{ii} assuming the environment is relatively stable. Hence, P_{bs} can be evaluated using path loss alone and by ignoring other channel uncertainties. However, other channel uncertainties such as Rayleigh fading and Shadowing are considered during the calculation of interference since reader locations are relatively farther away compared to a reader and a tag and since readers are power sources.

Interference caused by reader j at reader i is given as

$$I_{ij} = K_2 \cdot \frac{P_j}{r_{ij}^{2q}} \cdot 10^{0.1\zeta} \cdot X_{ij}^2 = g_{ij} \cdot P_j \tag{4}$$

where P_j is the transmission power of reader j, r_{ij} is the distance between the two readers, K_2 represents all other constant properties, $10^{0.1\zeta}$ corresponds to the effect of shadowing, and X is a random variable with Rayleigh distribution [8] to account for Rayleigh fading loss in the channel between reader j and reader i. After simplification, g_{ij} represents the channel loss from reader j to reader i. It is important to notice that since the interference actually occurs at the tag backscatter sideband, only power at that particular frequency needs to be considered. This factor is also accounted for in K_2 and g_{ij}.

Cumulative interference I_i at any given reader i is essentially the sum of interference introduced by all other readers plus the variance of the noise η

$$I_i = \sum_{j \neq i} g_{ij} P_j + \eta. \tag{5}$$

Given the transmission power and interference, the actual detection range of a reader is given by

$$r_{\text{actual}}^{4q} = \frac{K_1 \cdot P_i}{R_{\text{required}} \cdot I_i}. \tag{6}$$

Received SNR for a tag at a desired range r_d can be calculated as

$$R_{rd} = \frac{K_1 \cdot P_i}{r_d^{4q} \cdot I_i}. \tag{7}$$

Merging (6) and (7), we can calculate the actual detection range r_{actual} in terms of R_{rd} as

$$r_{\text{actual}} = r_d \left(\frac{R_{rd}}{R_{\text{required}}} \right)^{1/4q}. \tag{8}$$

For analysis purposes, we assume any tag within such a range to be successfully detected by the reader due to BER specification. If a reader is completely isolated, meaning no interference, a maximum range $r_{\max}$ can be achieved by using the maximum power $P_{\max}$ of a given reader. In a practical application, it is not possible to expect this maximum range due to interference even though maximum power is used. It is important to note from (8) that the detection range and SNR are interchangeable

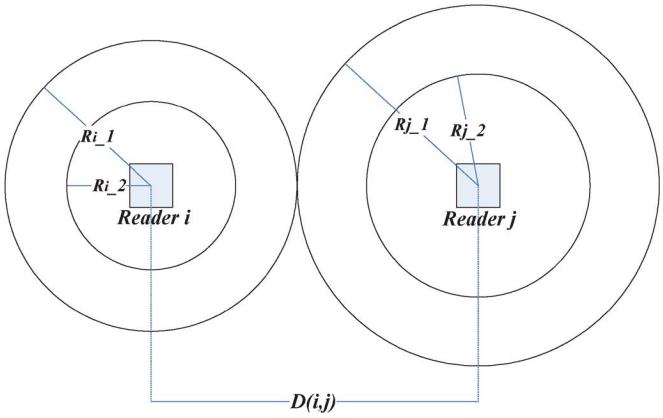

Fig. 1. Two-reader model.

and, therefore, our proposed algorithms attain the target SNR. By viable power control, both read rate and coverage can be achieved.

By substituting (3) and (4) into (2), the SNR expressed as a time-varying function for a particular reader is given by

$$R_i(t) = \frac{P_{bs}(t)}{I_i(t)} = g_{ii} \cdot P_i(t) \Bigg/ \left(\sum_{j \neq i} g_{ij}(t) P_j(t) + u_i(t) \right). \tag{9}$$

Notice that g_{ii} is considered to be a constant for a particular reader-tag link by assuming that the tag is stationary. If the desired range for the reader is defined as r_d which is less than $r_{\max}$, then we can define the SNR for the backscatter signal from a tag placed at a distance r_d to a reader as

$$\begin{aligned} R_{i-rd}(t) &= \frac{P_{bs-rd}(t)}{I_i(t)} \\ &= g_{ii-rd} \cdot P_i(t) \Bigg/ \left(\sum_{j \neq i} g_{ij}(t) P_j(t) + u_i(t) \right) \end{aligned} \tag{10}$$

where

$$g_{ii-rd} = \frac{K_1}{r_d^{4q}}. \tag{11}$$

Equation (10) provides the basic relationship among the SNR, output power of a particular reader under consideration and the output power of all readers through interference experienced in the network. This relationship is used throughout this paper to derive the power control algorithms.

B. Simple Two-Reader Model

To better understand the problem, a simple two-reader model is considered first. Given two readers i and j spaced $D(i,j)$ apart, each with the desired range R_{i_1} and R_{j_1}, respectively, are shown in Fig. 1. Readers must provide transmission powers P_i and P_j to achieve their respective desired range without considering interference. However, due to the interference introduced by each other, the actual detection range in fact decreases to R_{i_2} and R_{j_2}, respectively.

As a result of not achieving the SNR at a desired detection range due to interference, readers must attempt to increase their transmission power. If both readers increase their powers greedily, they will eventually reach the maximum power without achieving the desired range due to increased interference with output power. Further, the SNR target is not met and as a result the tags are not read even those that are in range. One could solve this problem by operating them in mutually exclusive time slots. However, as the number of readers increase, this strategy severely degrades each reader's average read time and detection range and eventually increases reading intervals.

A more appropriate solution is to balance the transmission power between the two readers in order to reach the equilibrium where multiple readers can achieve their respective read range. In the previous model, if reader i transmits at $P_{\max}$ and reader j is off, a read range greater than the targeted value of R_{i_1} can be achieved. On the other hand, there exists a power level at which reader j can transmit and still allow i to achieve read range R_{i_1}. This process can be applied in reverse to enable reader j to achieve its targeted range. Under such circumstances, the average read range of both readers is improved over the typical on and off cycle. Such a yielding strategy is required in dense reader networks where desired range may not be achieved by all the readers simultaneously. The effect of this improvement will be significant in dense networks due to the strategy. Section II-C details such a decentralized strategy.

C. Distributed Solution

In this paper, distributed power control scheme is introduced—adaptive power control (DAPC) and its implementation. DAPC involves systematic power updates based on local interference measurements at each reader. It also uses embedded channel prediction to account for the time-varying fading channel state for the next cycle. In Section III, we analytically show that the proposed DAPC scheme will converge to any target SNR value in the presence of channel uncertainties. For dense networks where the target SNR cannot be reached by all readers simultaneously, an addition *selective back-off* method is incorporated besides power updates introducing a degree of yielding to ensure that all readers achieve their desired range.

D. Standards

Implementing FHSS on readers has been explored in the past as a solution to the interference problem. While FHSS reduces the probability of interference, it is not a universal solution because of the differing spectral regulations over the world. In proposed work, frequency hopping is not considered. New standards [9] have been designed in dense reader networks by spectrally separating reader and tag modulation frequencies. However, subject to the transmit mask specifications and hardware implementations, substantial interference will still exist at the sideband frequencies of a tag in a highly dense reader network. The proposed work is not dependent upon any existing RFID standards or implementations and can be easily adapted to improve the performances of RFID reader networks.

III. DAPC

Distributed power control (DPC) protocols have been extensively studied in the field of wireless communication, including in *ad hoc* networks [13] and cellular networks [12]. Conceptually, power control in an RFID reader network is similar to these protocols. However, there are several fundamental differences between them due to the unique nature of the communication interface and RFID application. Moreover, a tag is not smart compared to a cell phone or a sensor node and, therefore, such schemes have to be modified for RFID applications.

First, the main goal of DPC in wireless communication is to conserve energy while maintaining desired quality of service (QoS) requirements. In [10]–[13], the authors propose different power updating schemes in order to maintain a target SNR threshold for successful communication. By contrast, the work proposed for RFID systems is to reduce interference introduced by others while maintaining read range requirements at each reader thereby achieving an optimal coverage for all readers and read rates. Second, DPC for *ad hoc* and cellular networks requires feedback signal between the transmitter and receiver.

In RFID reader networks, the reader acts both as a transmitter and receiver. Hence, the feedback is internal to the reader and does not result in any communication overhead. Third, in contrast to low-power wireless networks run on battery power, RFID readers in dense networks may not achieve the target SNR even at maximum power owing to the high levels of interference. Finally, in contrast with a connection oriented network where each node transmits only when it is needed, most RFID readers are required to be always on and transmitting in order to read the tags. Therefore, it is more difficult in distributing the channel access among all readers.

The proposed DAPC algorithm consists of two building blocks—*adaptive power update* and *selective back-off*. The goal of the *adaptive power update* is to achieve required SNR with an appropriate output power by correctly estimating the interference and any channel uncertainties. In dense networks, *selective back-off* forces high power readers to yield so that other readers can achieve required SNR. We now discuss these two building blocks of DAPC in depth.

A. Power Update Scheme

The development and the performance of DAPC are now demonstrated analytically. Differentiating the SNR (10) since the channel interference follows the time-varying nature of the channel, we get

$$R'_{i-rd}(t) = g_{ii-rd} \cdot \frac{P'_i(t)I_i(t) - P_i(t)I'_i(t)}{I_i^2(t)} \tag{12}$$

where $R'_{i-rd}(t)$, $P'_i(t)$, and $I'_i(t)$ are the derivatives of $R_{i-rd}(t)$, $P_i(t)$, and $I_i(t)$, respectively.

Applying Euler's formula, (12) can be transformed into discrete time domain as

$$\begin{aligned}\frac{R_{i-rd}(l+1)-R_{i-rd}(l)}{T} &= \frac{g_{ii-rd}\cdot P_i(l+1)}{I_i(l)T} \\ &\quad - \frac{g_{ii-rd}\cdot P_i(l)}{I_i^2(l)T} \\ &\quad \cdot \sum_{j\neq i} \left([g_{ij}(l+1)-g_{ij}(l)]\,P_j(l)\right. \\ &\quad \left. + g_{ij}(l)\,[P_j(l+1)-P_j(l)]\right).\end{aligned} \tag{13}$$

After the transformation, (13) can be expressed as

$$R_{i-rd}(l+1) = \alpha_i(l)R_{i-rd}(l) + \beta_i v_i(l) \tag{14}$$

where

$$\alpha_i(l) = 1 - \frac{\sum_{j\neq i} \Delta g_{ij}(l)P_j(l) + \Delta P_j(l)g_{ij}(l)}{I_i(l)} \tag{15}$$

$$\beta_i = g_{ii-rd} \tag{16}$$

and

$$v_i(l) = P_i(l+1)/I_i(l) \tag{17}$$

with the inclusion of noise, (14) is written as

$$R_{i-rd}(l+1) = \alpha_i(l)R_{i-rd}(l) + \beta_i v_i(l) + r_i(l)\omega_i(l) \tag{18}$$

where $\omega(l)$ is the zero mean stationary stochastic channel noise with $r_i(l)$ is its coefficient.

From (18), we can obtain the SNR at time instant $l+1$ as a function of channel variation from time instant l to $l+1$. The difficulty in designing the DAPC is that channel variation is not known beforehand. Therefore, α must be estimated for calculating the feedback control. Now define, $y_1(k) = R_{i-rd}(k)$, then (18) can be expressed as

$$y_i(l+1) = \alpha_i(l)y_i(l) + \beta_i v_i(l) + r_i(l)\omega_i(l). \tag{19}$$

Since α_i and r_i are unknown, (19) can be transformed into

$$\begin{aligned}y_i(l+1) &= [\alpha_i(l) \quad r_i(l)] \begin{bmatrix} y_i(l) \\ \omega_i(l) \end{bmatrix} + \beta_i v_i(l) \\ &= \theta_i^T(l)\psi_i(l) + \beta_i v_i(l)\end{aligned} \tag{20}$$

where $\theta_i^T(l) = [\alpha_i(l)\ r_i(l)]$ is a vector of unknown parameters and $\psi_i(l) = \left[\begin{smallmatrix} y_i(l) \\ \omega_i(l) \end{smallmatrix}\right]$ is the regression vector. Now selecting feedback control for DAPC as

$$v_i(l) = \beta_i^{-1}\left[-\hat{\theta}_i(l)\psi_i(l) + \gamma + k_v e_i(l)\right] \tag{21}$$

where $\hat{\theta}_i(l)$ is the estimate of $\theta_i(l)$, then the SNR error system is expressed as

$$\begin{aligned}e_i(l+1) &= k_v e_i(l) + \theta_i^T(l)\psi_i(l) - \hat{\theta}_i^T(l)\psi_i(l) \\ &= k_v e_i(l) + \tilde{\theta}_i^T(l)\psi_i(l)\end{aligned} \tag{22}$$

where $\tilde{\theta}_i(l) = \theta_i(l) - \hat{\theta}_i(l)$ is the error in estimation.

From (22), it is clear that the closed-loop SNR error system is driven by channel estimation error. If the channel uncertainties are properly estimated, then SNR estimation error tends to be zero, therefore, the actual SNR approaches the target value. In the presence of error in estimation, only boundedness of error in SNR can be shown. Given the closed-loop feedback control and error system, we can now advance to the channel estimation algorithms.

Consider now the closed-loop SNR error system with channel estimation error $\varepsilon(l)$ as

$$e_i(l+1) = k_v e_i(l) + \tilde{\theta}_i^T(l)\psi_i(l) + \varepsilon(l) \tag{23}$$

where $\varepsilon(l)$ is the error in estimation which is considered bounded above $\|\varepsilon(l)\| \leq \varepsilon_N$, with ε_N a known constant.

Theorem 1: Given the previous DPC scheme with channel uncertainties, if the feedback from the DPC scheme is selected as (21), then the mean channel estimation error along with the mean SNR error converges to zero asymptotically, if the parameter updates are taken as

$$\hat{\theta}_i(l+1) = \hat{\theta}_i(l) + \sigma\psi_i(l)e_i^T(l+1) - \Gamma \left\| I - \psi_i^T(l)\psi_i(l) \right\| \hat{\theta}_i(l). \tag{24}$$

Then the mean error in SNR and the estimated parameters are bounded

$$\sigma \|\psi_i(l)\|^2 < 1 \tag{25}$$

$$0 < \Gamma < 1 \tag{26}$$

$$k_{v\max} < 1/\sqrt{\delta} \tag{27}$$

where

$$\delta = \eta + 1 \Big/ \left(1 - \sigma \|\Psi_i(l)\|^2\right) \left[\Gamma^2 \left(1 - \sigma \|\Psi_i(l)\|^2\right)^2 + 2\sigma\Gamma \|\Psi_i(l)\|^2 \left(1 - \sigma \|\Psi_i(l)\|^2\right)\right] \tag{28}$$

and σ is the adaptation gain.

Note: The parameters σ, η, and δ are dependent upon the desired SNR value with time.

Proof sketch: In the proof, a Lyapunov function candidate is selected and is shown to have stability in the mean sense of Lyapunov provided the conditions (25) and (27) hold. Hence, according to a standard Lyapunov extension [16], the SIR error $E[e_i(l)]$ is bounded for all $l \geq 0$ and the upper bound on the mean SIR error is given by

$$E\left(\|e_i(l)\|\right) > 1/\left(1 - \sigma k_{v\max}^2\right) \left[\gamma k_{v\max} + \sqrt{\rho_1 \left(l - \sigma k_{v\max}^2\right)}\right] \tag{29}$$

where

$$\rho_1 = \rho + \frac{1}{\sigma}\frac{\Gamma}{2-\Gamma}\left(1 - \sigma \|\theta(l)\|^2\right)^2 \theta_{\max}^2. \tag{30}$$

It is also shown that

$$E\left(\left\|\tilde{\theta}_i(l)\right\|\right) > \left(\Gamma(1-\Gamma)\theta_{max} + \sqrt{\Gamma^2(1-\Gamma)^2\theta_{max}^2 + \Gamma(2-\Gamma)\Theta}\right) \Big/ \left(\Gamma(2-\Gamma)\right) \tag{31}$$

where

$$\Theta = \left[\Gamma^2\theta_{\max}^2 + \sigma\rho_1 \Big/ \left(1 - \sigma \|\Psi_i(l)\|^2\right)^2\right] \tag{32}$$

and

$$\rho_1 = \rho + \frac{\gamma^2 k_{v\max}^2}{\left(1 - \delta k_{v\max}^2\right)}. \tag{33}$$

In general, as long as (25) and (27) are satisfied and either (29) or (30) holds, according to the standard Lyapunov extension theorem [16], this demonstrates that the tracking error and the error in weight estimates are bounded without the need for any PE condition on the inputs. The proof is detailed in [16].

Remarks:

1) Note that for practical purposes, (29) and (30) can be considered as bounds for $\|e_i(l)\|$ and $\|\widetilde{\theta}_i(l)\|$.
2) Note that the parameter reconstruction error bound ε_N and the bounded channel disturbances d_M increase the bounds on $\|e_i(l)\|$ and $\|\widetilde{\theta}_i(l)\|$ in a very interesting way.

B. Selective Back-Off

In a dense reader environment where multiple readers are deployed for coverage, it is inconceivable that all readers are able to achieve their target SNR together due to severe congestion which affects both read rates and coverage. These readers will eventually reach maximum power as a result of the *adaptive power update*. This demands a time-based yielding strategy of some readers to allow others to achieve their target SNR.

Whenever the reader finds the target SNR is not achievable at the maximum power, meaning the interference level is too high in the network, it should back-off to a low output power for a period of time. Since interference is a locally experienced phenomenon, multiple readers will face this situation and they will all be forced to back off. The rapid reduction of power will result in significant improvement of SNR at other readers. After waiting for the back-off period, a reader will return to normal operation and attempt to achieve the target SNR. The process is repeated for every reader in the network. To fairly distribute the channel access among all congested readers, certain quality measurements must be made for all readers in the back-off scheme. The *selective back-off* scheme uses the percentage of time a reader has achieved its desired range with respect to the quality control parameter to ensure fairness.

After backing off, each reader must wait for a time duration τ_w. In order to illustrate the effect of back off, τ_w is defined as a logarithm function of the percentage of time ρ a reader has attained the required SNR. A neglected reader will exit back-off mode quickly and attain the required SNR while other readers in the vicinity fall back. The calculation of τ_w is given by

$$\tau_w = 10 \cdot \left[\log_{10}(\rho + 0.01) + 2\right]. \tag{34}$$

Using the previous equation, a reader with ρ equals 10% will wait for ten time intervals while the waiting time for ρ of 100% equals 20. A plot of waiting time τ_w versus ρ is presented in Fig. 2.

The back-off policy will cause negative changes in interference, and hence does not adversely affect the performance of

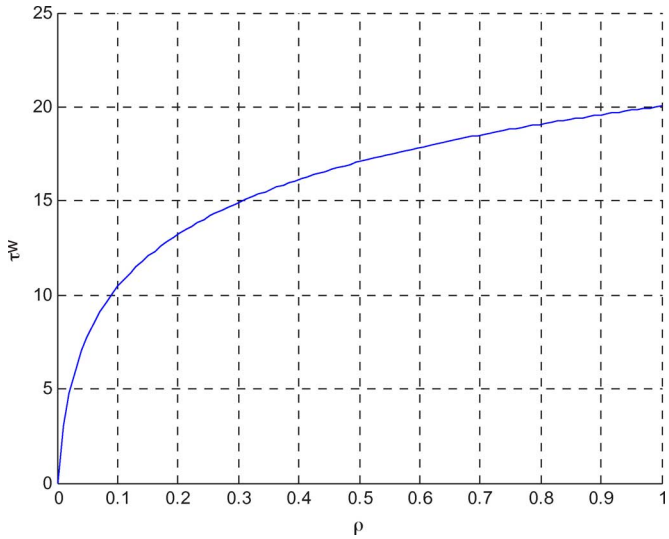

Fig. 2. Selective back-off function plot.

TABLE I
SELECTIVE BACK-OFF PSEUDOCODE

```
If reader is not in back-off mode
   If Pnext == Pmax
                change reader to back-off mode
                    initialize wait time τw
If reader is in back-off mode
   Set Pnext = Pmin
                          decrease τw
      If τw == 0
                          reader exit back-off mode
```

the adaptive power update. A detailed pseudocode for implementing *selective back-off* is given in Table I.

C. DAPC Implementation

DAPC can be easily implemented at the MAC layer of the RFID reader and MAC implementation is not covered in detail in this paper. The algorithm requires two parameters to be known initially. These are the desired range r_d, and target SNR R_{required}.

Proposed DAPC can be seen as a feedback between the transmitter and receiver units of a reader. A block diagram of the implementation is shown in Fig. 3. The detailed description of the algorithm implementation is presented as follows.

1) Power update block at the receiver unit of a reader obtains sensed interference $I(l)$.
2) In the power update block, based on r_d, R_{required}, and current power $P(l)$, the current SNR $R_{i-rd}(l)$ is calculated.
3) $R_{i-rd}(l)$ is compared to R_{required}, and percentage of time achieving required SNR, ρ is calculated and recorded.
4) Based on (24), the channel is estimated for the next time step $l+1$, and the power for $P(l+1)$ is also calculated using the feedback control (21).
5) $P(l+1)$ is then limited to maximum power $P_{\max}$, if the $P(l+1)$ greater than $P_{\max}$, the *selective back-off* scheme is triggered, otherwise, $P(l+1)$ is used as the output power for the next cycle.

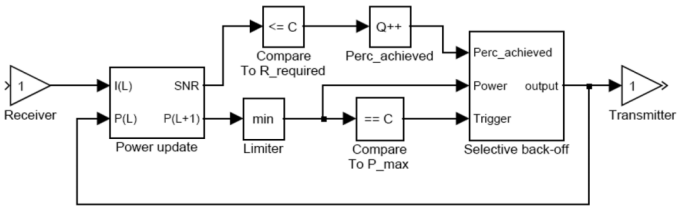

Fig. 3. Block diagram for DAPC implementation.

6) The *selective back-off* block follows the algorithm provided in Section III-C and restricts the final output power for the next cycle.

IV. SIMULATION SETUP

The simulation environment is set up in MATLAB. The full model of DAPC is implemented for comparison and compared with probabilistic scheme.

A. Reader Design

Reader power is implemented as a floating point number varying from 0 to 30 dBm (1 W) as per FCC regulation. For error-free detection, the reader should maintain a target SNR of 14 ($\sim$11 dB). Other system constants are designed so that the maximum read range of a reader in isolated environment is 3 m. Interference experienced at any reader is calculated based on a matrix consisting of power and positions of all other readers plus the channel variation g_{ij}. A desired range of 2 m is specified based on the worst case analysis.

For proposed DAPC, *power update* parameters Kv and σ are both set to 0.001. The results are compared with another scheme referred to as probabilistic power control (PPC) method [15]. Recall that the read range of a particular reader is dependent on its transmission power and the interference experienced which is a function of powers of all other readers. If reader powers follow certain probability distribution, the distribution of read ranges for each reader is a function of these power distributions

$$F(r_i) = f_i\left(F(P_1), \ldots, F(P_n)\right) \tag{35}$$

where $F(r_i)$ is the cumulative density function of read range of reader i, and $F(P_i)$ is the cumulative power density function of reader i. Performance metrics including mean read range μ_r and percentage of time ρ achieving desired range r_d characterized the read range distribution $F(r_i)$

$$F(r_i) = g_i(\mu_r, \rho). \tag{36}$$

To achieve targeted characteristics on the read range distribution, we need to modify the power distribution freely. Beta distribution, demonstrated is specifically chosen for this reason; by specifying the shape variables α and β, one can change the cumulative density function in the domain from 0 to 1 (0% to 100% power). By changing these two parameters, we can control the power distribution and thus attempt to achieve desired targets on the read range distribution in (35). For proposed PPC, both

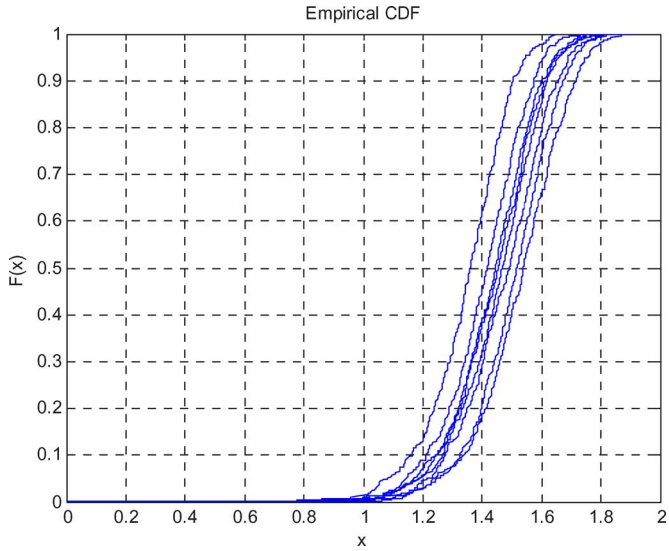

Fig. 4. Cumulative density functions of the read range.

$Beta(0.1, 0.1)$ and $Beta(2, 2)$ distributed are implemented in simulation.

B. Simulation Parameters

For both models, random topologies are generated in order to emulate a denser network with a suitable number of readers. The RFID network with a suitable density for a given scenario is created by placing the readers with the minimum distance between them and the maximum area under test. The minimum distance between any two readers is varied from 4 to 14 m and the maximum size of the coordinate is adjusted accordingly. The number of readers is changed from 5 to 60 for creating denser network and to test the scalability of the proposed schemes. Each simulation scenario is executed for 10 000 iterations.

C. Evaluation Metrics

To demonstrate the typical performance of the reader network, the cumulative range distribution of a reader can be plotted. In Fig. 4, the cumulative density function $F(x)$ of read range x for a reader using DAPC is plotted. From this plot, we can observe the minimum and maximum detection range as well as the percentile of attaining certain ranges. To evaluate the performances of the proposed algorithms, the following metrics: average read range, percentage of time attaining desired range, average output power, and average interference experienced are evaluated across all readers for each scenario and simulation results are given.

V. DAPC Hardware Implementation

The DAPC hardware implementation is made generic and applicable to any *ad hoc* wireless networking scenario and does not restrict it to RFID alone. It is only intended to demonstrate the working principles of the DAPC on a generic wireless test platform. Here, instead of using RFID reader antennas, we have used UMR Mote hardware. The objective is to show that the desired SNR can be obtained in the presence of channel uncertainties. Moreover, this paper discusses in detail about the design

TABLE II
DAPC Pseudocode

```
Packet reception
  If Receiver
    Calculate SNR = Signal Strength / Noise Strength
    Channel estimation algorithm
    Calculate transmitter power p_t for next packet
    Feedback packet including power p_t
  If Transmitter
    Extract feedback power p_t
    Transmit next packet using p_t
```

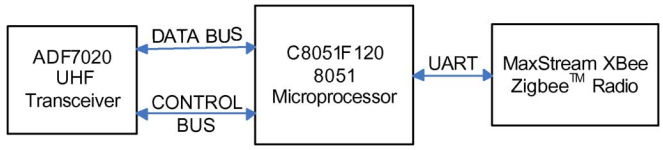

Fig. 5. Hardware block diagram.

specifications and requirements. The results of the implementation of DAPC tested as an RFID platform are presented as a specific application.

The proposed DAPC should be implemented at the medium access control (MAC) layer since it is specific to the connection and requires physical access to certain baseband parameters, such as RSSI reading and output power. A detailed description of the DAPC MAC is discussed in Section V-B. We will now discuss the implementation in terms of hardware and software issues. DAPC pseudocode is given in Table II.

A. Hardware Architecture

In this section, an overview on the hardware implementation of the DAPC protocol is given. First, a customized wireless communication test platform for evaluating wireless networking protocols is presented. A detailed description of capabilities and limitations of the test platform is discussed.

1) Wireless Networking Test Platform: In order to evaluate various networking protocols, a UHF wireless test platform is designed based on the UMR/SLU Generation-4 Smart Sensor Node (G4-SSN). Silicon Laboratories 8051 variant microprocessors was selected for its ability to provide fast 8-bit processing, low-power consumption, and ease of interfacing to peripheral components. ADF7020 ISM Band transceiver was employed as the underlying physical radio for its ability to provide precise control in frequency, modulation, power, and data rate. A Zigbee compliant Maxstream XBee RF module was also employed as a secondary radio unit providing alternative wireless solutions. The former is suitable for low level protocol development at the MAC or baseband level, whereas the latter is great for implementing high level routing and scheduling protocols. Using either the ADF7020 or the Zigbee radio interface, wireless networks can be formed and various networking protocols can be implemented for evaluation. A block diagram of the hardware setup is shown in Fig. 5.

a) Generation-4 Smart Sensor Node (G4-SSN): The G4-SSN, was originally developed at UMR and subsequently updated at St. Louis University. The G4-SSN has various abilities in sensing and processing. The former include strain gauges,

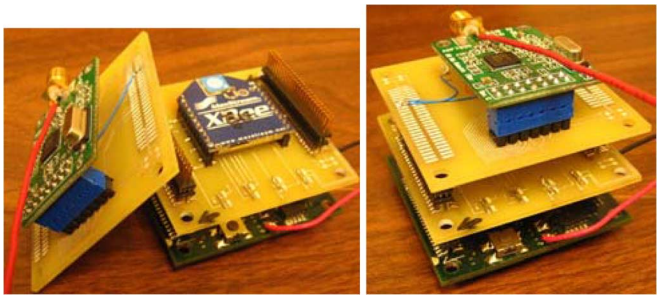

Fig. 6. Gen-4 SSN with (left) Zigbee layer (right) ADF7020 layer.

TABLE III
G4-SSN CAPABILITIES

	Ic @ 3.3V [mA]	Flash Memory [bytes]	RAM [bytes]	ADC Sampling Rate [kHz]	Form-Factor	MIPS
G4-SSN	35	128k	8448	100 @ 10/12-bit	100-pin LQFP	100

TABLE IV
ADF7020 CAPABILITIES

Features	Capabilities
Frequency Bands	431MHz ~ 478MHz & 862MHz ~ 956MHz
Data rates	0.15kbps to 200kbps
Output power	-16dBm to +13dBm in 0.3dBm steps
RSSI	6-bit Digital read back
Modulation	FSK, ASK, GFSK
Power Consumption	19mA in receive, 28mA in transmit (10dBm)

accelerometers, thermocouples, and general A/D sensing. The latter includes analog filtering, CF memory interfacing, and 8-bit data processing at a maximum of 100 MIPS. These features provide a solid application level variability and have been utilized in pervious works [17]. Moreover, the stackable connection easily allows for new hardware development. As seen in Fig. 6, the Zigbee radio and ADF7020 radio stack can be used together, therefore, allowing multiple radio interfaces.

As shown in Table III, the G4-SSN provides powerful 8-bit processing, a suitable amount of RAM, and a low-power small form-factor.

b) ADF7020 ISM band transceiver: ADF7020 ISM band transceiver is used as the physical layer for the implementation for DAPC protocol. The major advantage given by the ADF7020 is the freedom in controlling various physical layer properties, including operating frequency, output power, data rate, and modulation scheme as given in Table IV. These features are essential in evaluating new wireless protocols which require physical level access. In the DAPC implementation, direct access RSSI reading and output power are used. In addition, the low power consumption of this transceiver is suitable for embedded sensor network applications.

2) Limitations: Hardware implementation of any algorithm is constrained by the limitations of the hardware. With a single-chip software layered architecture, the microprocessor must simultaneously handle data communication with radio transceivers, internal processing, and applications. Therefore, the 8-bit processing power limits the data rate at which the radio transceivers can operate at. Currently, a maximum data rate of 48 kb/s is successfully tested. Quantization is another issue faced in hardware and cannot be avoided. Quantization means that the hardware does not provide enough precision as desired by the algorithm, such as in calculation, analog-to-digital or digital-to-analog converter. In the implementation of DAPC, signal strength reading is only accurate up to 0.5 dB and power control is limited to 0.3-mW steps. These limitations must be treated to reduce the effects on the algorithm.

3) RF Setup: The wireless channel for the DAPC implementation is chosen to be similar to the case in RFID systems. The nodes will operate at the central frequency of 915 MHz with 20 kHz channel bandwidth. In order to test the performance of only DAPC, no other medium access control is used. The data rate is setup at 12 kb/s using FSK modulation with no encoding method. The output power at the transmitter can vary from -16 dBm to $+13$ dBm at 0.3 dB increment.

B. Software Architecture

A layered networking architecture is considered for the G4-SSN wireless test platform. This would allow easier future implementations and protocol evaluations. A block diagram of the layered software architecture is shown in Fig. 7. In this section, a detailed description of the baseband controller and DAPC MAC design is given.

1) Frame Format: Frame format used for DAPC implementation is shown in Fig. 8. The physical layer header is composed by a series of SYNC bytes and a preamble sequence. The SYNC bytes which are used to synchronize the transmitter and receiver clock should be a dc-free pattern such as 10101010... pattern. The preamble sequence is a unique pattern indicating the beginning of a packet and must be universal to all nodes in the network. The ADF7020 provides hardware preamble detection and interrupt source to the microprocessor.

The preamble is followed by the MAC header. The length of the MAC header can be programmable using its first byte, therefore, allowing multiple extensions for the future. For DAPC, only transmission power field is required. After the MAC header, data and CRC are transmitted.

2) Baseband Controller: A baseband controller is implemented to interface with the physical layer as shown in Fig. 9. It also provides an API for higher layers to access all functionalities offered by radio transceiver. In the implementation of DAPC MAC, only RSSI read back and power control are used. Other options are available and can be utilized easily for future implementations of different protocols.

a) Operation modes: The baseband controls the radio in three operation modes, *Transmit*, *Receive* and *Idle*, which is handled by the Tx/Rx state machine. The radio should always operate in idle mode unless a packet is ready for transmission or a preamble is detected indicating the beginning of a packet reception.

i) ***Idle mode***: In *Idle* mode, the radio is still listening to the channel, however, any incoming data from the radio is ignored.

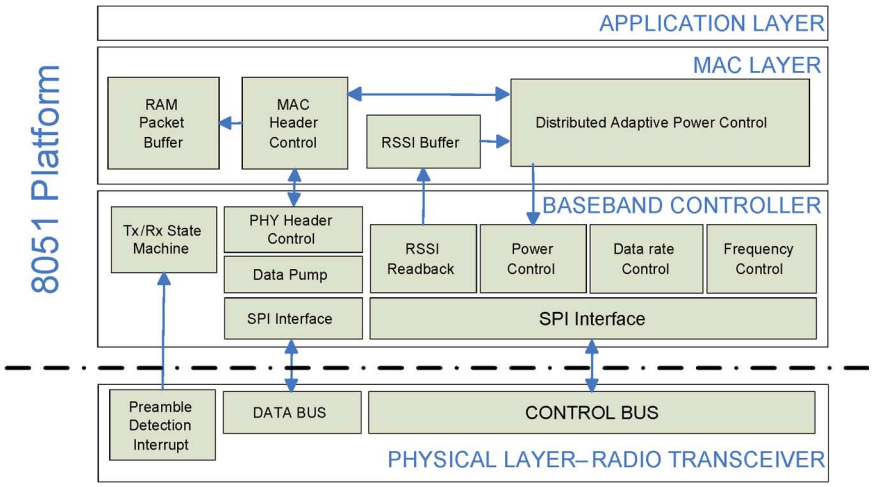

Fig. 7. Software architecture.

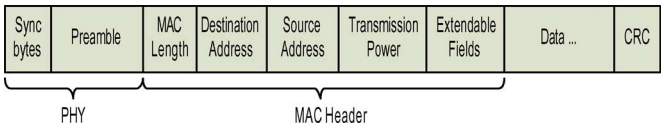

Fig. 8. Protocol frame format.

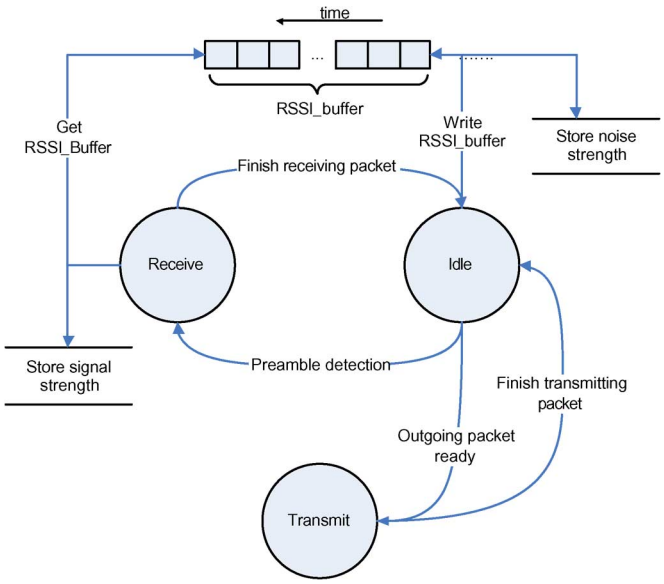

Fig. 9. Baseband flow chart.

ii) ***Receive mode***: During *Idle* mode, when a preamble is detected by the radio, an interrupt is sent to the microprocessor. Upon interrupt, the baseband switches to *Receive* mode and begins buffering incoming bytes; the length of the packet is prefixed between the transmitter and receiver.

iii) ***Transmit mode***: When a packet is ready for transmission, the baseband switches to *Transmit* mode, appends the preamble, and sends out the entire packet with no interruptions.

b) RSSI reading: The implementation of DAPC requires RSSI readings to calculate the SNR for every packet. In order

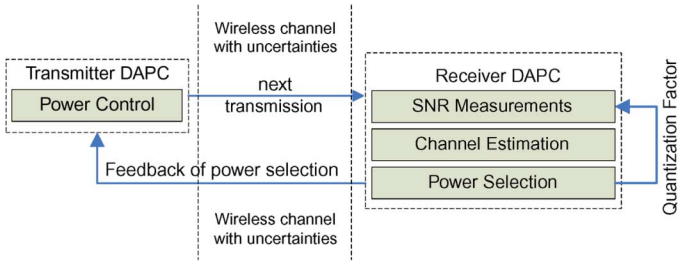

Fig. 10. DAPC in control loop.

to provide accurate SNR values, RSSI readings are taken at the reception of every byte. When radio is in *Idle* mode, any incoming data is discarded, however, RSSI value is still recorded every 8-bits. To separate preamble from noise, a small *rssi_buffer* stores the past N values of RSSI, where N equals to the length of preamble bytes. Any reading beyond N is averaged as the *noise_power*. After the radio enters the *Receive* mode, RSSI is recorded and averaged along with the values in *rssi_buffer* to provide *signal_power*. A flow chart diagram of the mode switching and RSSI reading is shown in Fig. 10.

3) DAPC MAC Controller: Fig. 10 illustrates the block diagram representation of the proposed DAPC control loop inside a transmitter and receiver.

At the receiver side, signal strength P_i and noise level I_i, and, therefore, the SNR R_i, are measured at the reception. Output power at the transmitter, P_t is known from the previous calculation. Given P_t and P_i, the channel attenuation g_{ii} for the previous transmission can be calculated. Now, update θ_i using (24), and calculate P_t using (21). P_t is then embedded into the MAC header of the next outgoing packet to the corresponding transmitter. At the reception of the next packet, the cycle begins again.

At the transmitter side, DAPC must extract the power information from the MAC header and inform the baseband to transmit P_t for the next outgoing packet to the corresponding receiver. In hardware implementation, especially in digital systems, a quantization factor should be introduced since the hardware may not provide the precision for output power which

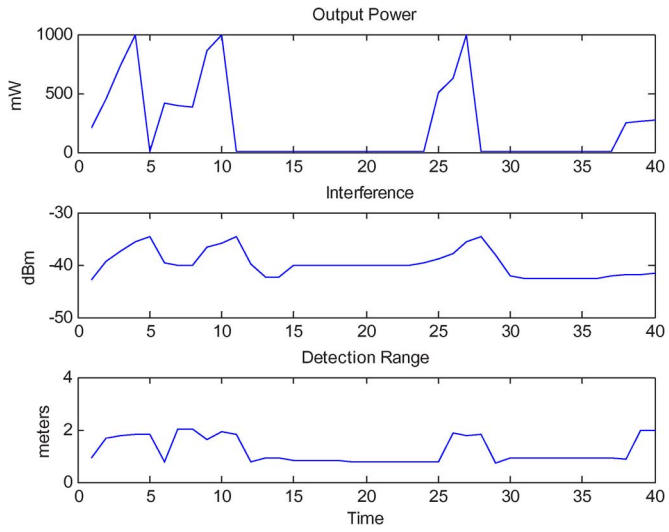

Fig. 11. Output power, interferences, and detection range versus time in seconds.

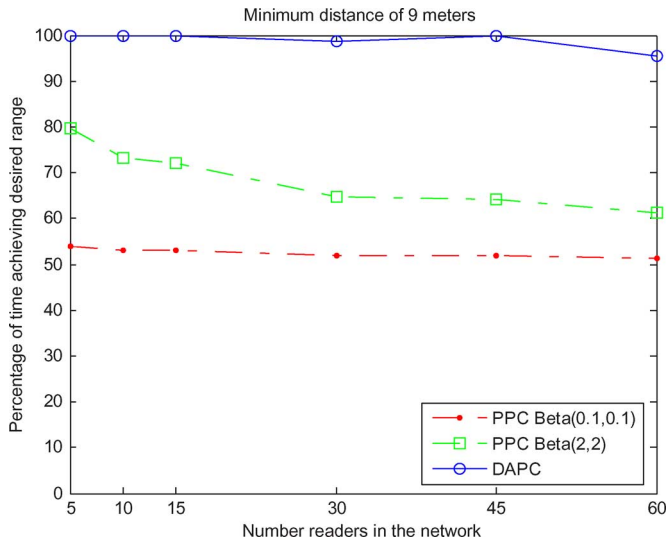

Fig. 12. Number of readers versus percentage of time achieving desired range.

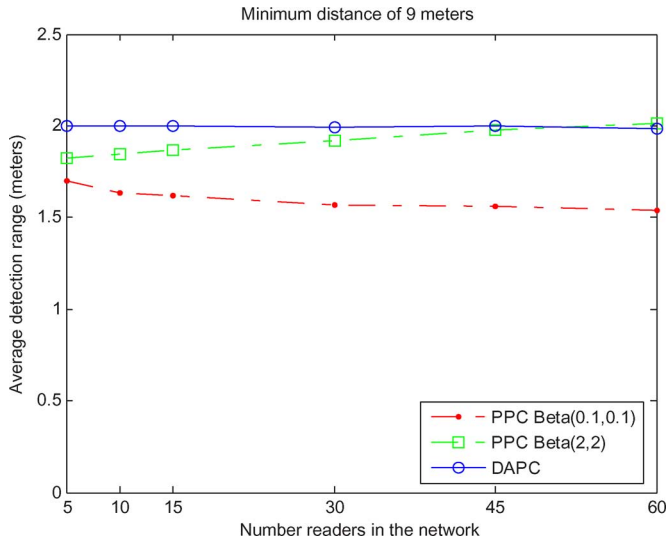

Fig. 13. Number of readers versus average detection range in meters.

DAPC desires. The quantization factor is simply the ratio between the actual $P_{t'}$ and desired transmission power P_t. This ratio is divided by the next power calculation to improve estimation accuracy and maintain system stability.

VI. Results and Analysis

A. Simulation Results

In Fig. 11, the output power, interference level, and detection range versus time at a particular reader are plotted for DAPC in a dense network. It is seen that DAPC attempts to achieve the desired range by increasing power, however the interference level is too high and, therefore, the reader reaches maximum power and enters selective back-off scheme. It is also observed that as the reader backs off to low power value, the interference level increases meaning that other readers are taking the advantage and accessing the channel. This plot also demonstrates the changes in back-off time corresponding to desired range achievement, for example, time interval 12 to 24 s and 28 to 37 s.

The analysis of performances in sparse networks is discussed first. With the minimum distance of 9 m between any two readers, the average percentage of time ρ attaining desire range across all readers is presented in Fig. 12. Note that each reader has a maximum detection range of 3 m without interference and the desired range is set to 2 m in the presence of multiple readers. DAPC is observed to have superior performances over the two PPC algorithms for this sparse network. DAPC converges to 100% desired range achievement with the appropriate parameter estimation and closed-loop feedback control described in Section III.

The results justify the theoretical conclusions. It is also shown that $Beta(2,2)$ performs better than $Beta(0.1,0.1)$ in terms of ρ. With $Beta(2,2)$ distribution, every reader will be on and transmitting at medium power most of the time. With sparse networks and small interferences, the medium power overcomes the interference produced and, therefore, achieving desired range. In contrast, $Beta(0.1,0.1)$ has a 30% probability being off, therefore, the probability of attaining desired range will be low.

In Fig. 13, considering the average detection range for the same scenario, DAPC converges to the 2-m desired range and outperforms both PPC algorithms. We can also observe the average power level used for each algorithm in Fig. 14. Since the mean for both $Beta(2,2)$ and $Beta(0.1,0.1)$ is 0.5, the average reader output power lays at 500 mW, which is half of the maximum power. Meanwhile, DAPC is able to dynamically adjust its output power to find the optimal level for which desired range can be achieved as the size of the network varies.

Performance of the power control schemes in denser networks is now analyzed. For network with minimum distance of 6 m, the desired range is not attainable by all readers since the transmission power is not able to overcome the interference forcing the yielding strategy of each algorithm to test. The detection range and percentile versus number of readers are presented in Figs. 15 and 16, respectively. As the number of readers

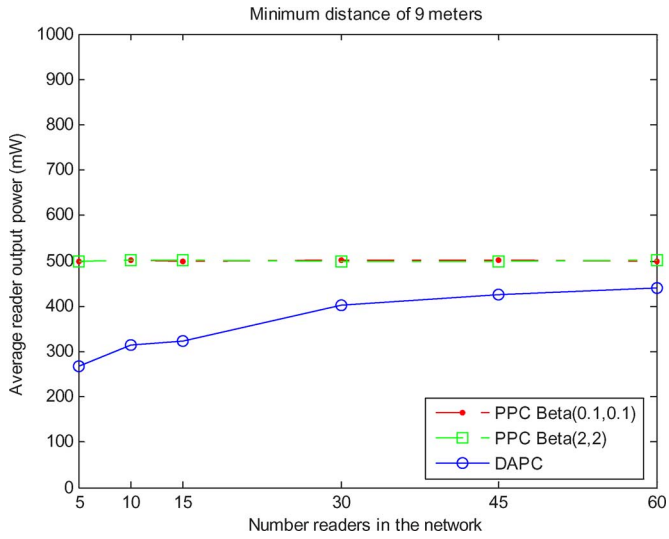

Fig. 14. Number of readers versus average output power per reader.

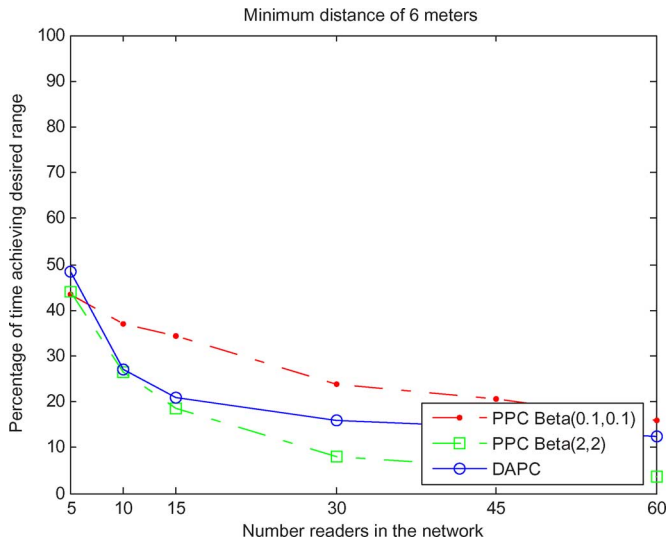

Fig. 15. Number of readers versus percentage of time achieving desired range.

increases, the overall interference in the network will also increase. Consequently, the percentage of time ρ a reader attains its desired range will drop as shown in Fig. 15.

It is observed that PPC with $Beta(0.1, 0.1)$ offers the best performances in terms of ρ. This is because on average 30% of the readers will be switched off for each time interval while for the other 30% they transmit at full power. Hence, readers in full power have great probability in attaining the desired range, whereas the average detection range is sacrificed for this achievement. The relatively poor performance in average detection range compared to DPC and PPC $Beta(2, 2)$ can be observed in Fig. 7.

While the percentage of time achieving a target range is low for $Beta(2, 2)$, it provides the best average detection range out of all three algorithms. DAPC with selective back-off scheme finds a balance between the two evaluation metrics. These show that there is a tradeoff between percentage time achieving the target range and average detection range achieved.

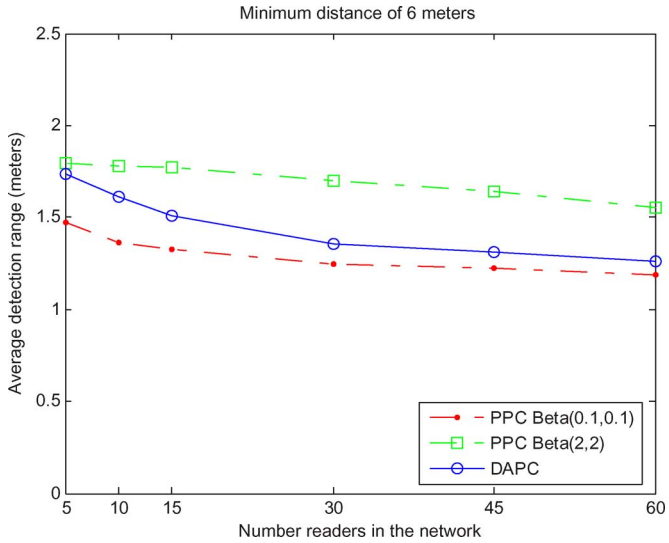

Fig. 16. Number of readers versus average detection range.

B. Hardware Implementation Results

In this section, hardware implementation results for DAPC are presented. Various experiments are executed to create channel interferences in order to thoroughly evaluate the performance of DAPC. Due to range and power limitations, the SNR for the test platform can reach to a maximum of 80 dB. Therefore, the system control parameter k_v and σ are very small and selected as 1e-15 and 0.01, respectively. Note that the experiments are conducted under normal office environments.

In general, a paired connection between a transmitter and receiver is established. The transmitter sends a 100-byte packet to the receiver every 500 ms. The receiver sends the reply with a 100-byte packet immediately after reception. This also indicates that the power update rate is 2 times/s. Essentially, the nodes act as transmitters and receivers, and DAPC is implemented on both of them. The working ranges for the experiments are usually within 5 m. DAPC results are also presented for the RFID scenario where the DAPC feedback loop is internal to the reader based on observed interference.

1) Path Loss Effect: In this setup, a paired connection is established. The receiver was slowly moved towards the transmitter and then taken away. The desired SNR for the receiver is set at 40 dB. Fig. 17 demonstrates the performance of DAPC. In red, the SNR at the receiver is plotted. In blue, the output power of the transmitter is plotted. The receiver SNR was kept very closely to the target SNR. We can clearly see that at packet number 65, the receiver starts moving close to the transmitter resulting a reduction in the power level. At the 180th packet, the radio had been moved back to its original location and the output power for the transmitter has increased to provide required SNR. This experiment shows that DAPC accurately estimate the channel loss g_{ii} in a noninterfered environment.

2) Slowly Varying Interference: In this experiment, a paired connection between a transmitter and a receiver is setup. At the same time, a constant interfering source is introduced to alter the channel with small variations per step. The time varying transmission power for the interfering source is displayed in Fig. 18. The transmission power for the interferer varies from -16 dBm

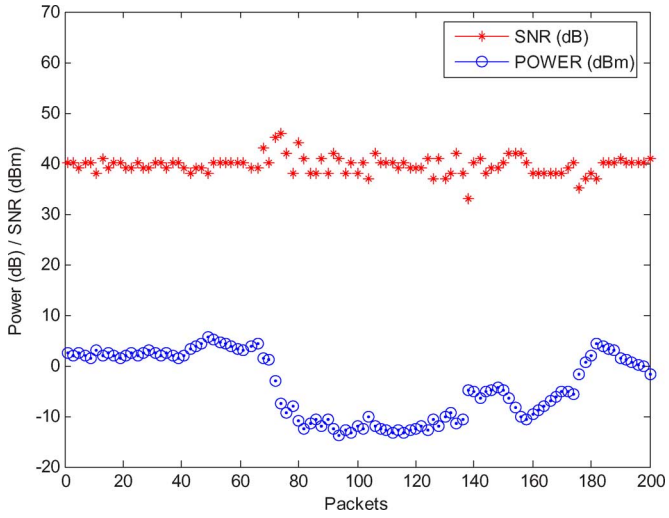

Fig. 17. Receiver SNR and transmitter power corresponding to channel uncertainties due to path loss.

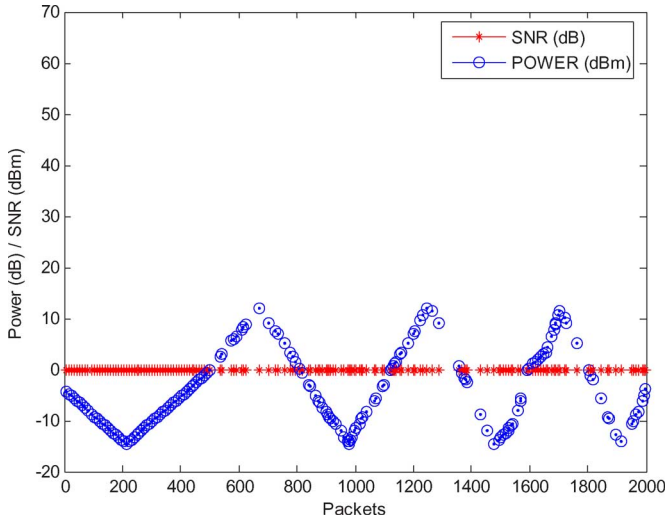

Fig. 18. Power variation of a slow changing interferer.

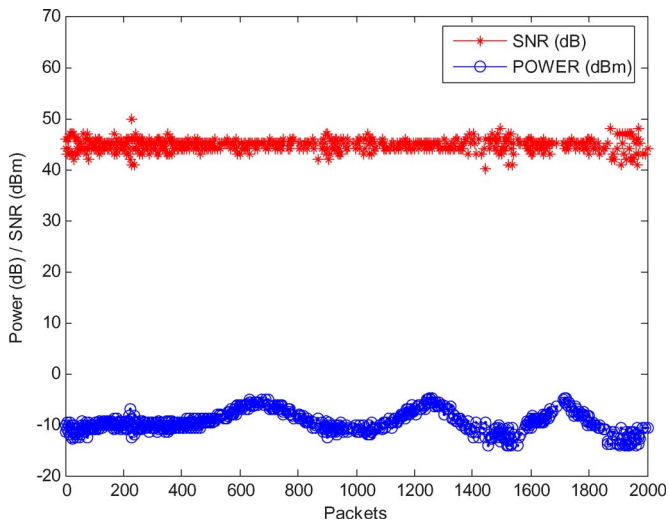

Fig. 19. Receiver SNR and transmitter power corresponding to channel uncertainties from a slow changing interferer.

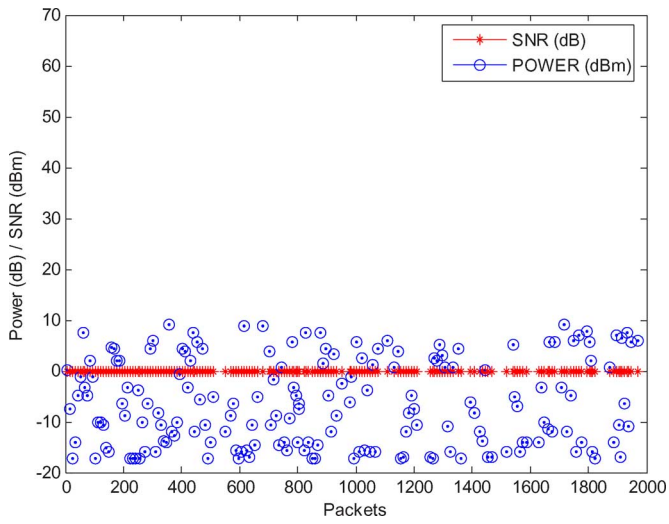

Fig. 20. Power variation of an interferer with random output power.

to 13 dB at a slow rate. Note that the rate for power update at the receiver is three times faster then rate of change of output power on the interferer.

At desired SNR value equal to 45 dB, we can observe that the SNR seen at the receiver is obtained very closely to the desired value. In blue, the output power at the transmitter is plotted. It shows that the change in transmitter power follows the power pattern of the interferer (see Fig. 19).

3) Abruptly Changing Channel With Slow Update: The setup here is the same as the previous experiment except that the interferer varies the transmission power randomly. The rate for the power update is three times faster then the rate of the interferer. This is considered as a very brutal interferer. The interference level is shown here in Fig. 20.

In Fig. 21, we can observe that the SNR at the receiver is not very well leveled comparing to a slowly varying channel due to the vast brutal interferer. However, it is still kept at an acceptable margin around 45 dB.

4) Abruptly Changing Channel With Fast Update: In this setup, the same interferer is used as the previous experiment. However, the rate for the power update is now 10 times faster then the interferer. With the desired SNR equal to 45 dB, we can observe that the SNR at the receiver performs very well with a faster update rate (see Fig. 22).

5) DAPC for RFID Applications: A simplified DAPC for passive RFID systems is also presented. In such system, RFID tags harvest energy from the RFID readers to power internal circuits and obtain communication. Readers operating in the same frequency interferer with the others resulting reduced detection range and read rate. In addition, since the tags are at low cost, any intelligent power control must be designed on the reader side only. Since the reader and tag range is relatively stationary and short in distance, interference by others is considered as the main source for channel uncertainties in RFID systems. Therefore, by assuming g_{ii} in (11) to be constant, the DAPC feedback

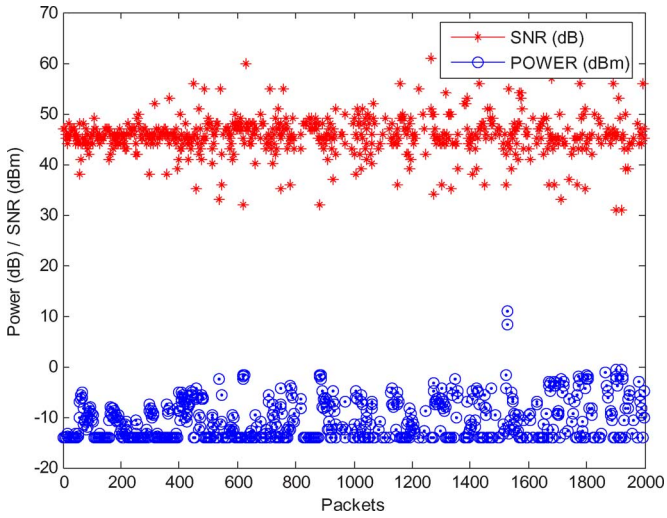

Fig. 21. Receiver SNR and transmitter power level corresponding to channel uncertainties from a brutal interferer—slow power update.

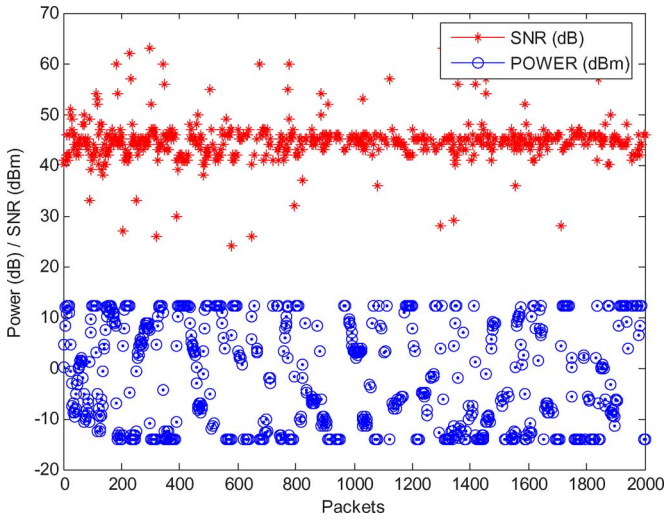

Fig. 22. Receiver SNR and transmitter power level corresponding to channeluncertainties from a brutal interferer—fast power update.

loop can be internal to the reader and only interference measurements are necessary. Received SNR can be directly converted into detection range and measure system performances.

RFID reader networks with four readers are implemented using the G-4SSN setup. The desired SNR for the readers is at 10 dB and a channel attenuation between the tag and reader is assumed to be 40 dB (g_{ii}). First, a system with no power control scheme is tested and the output power of all four readers is set to be -2 dBm. In Fig. 23, the performances of all four readers are shown and it is clear that two of the readers never achieve desired SNR and the others with very unstable SNR.

A network of readers with DAPC implementation is then tested in the same setup as the uncontrolled case. As shown in Fig. 24, all four readers reach the desired SNR of 10 dB at various power levels.

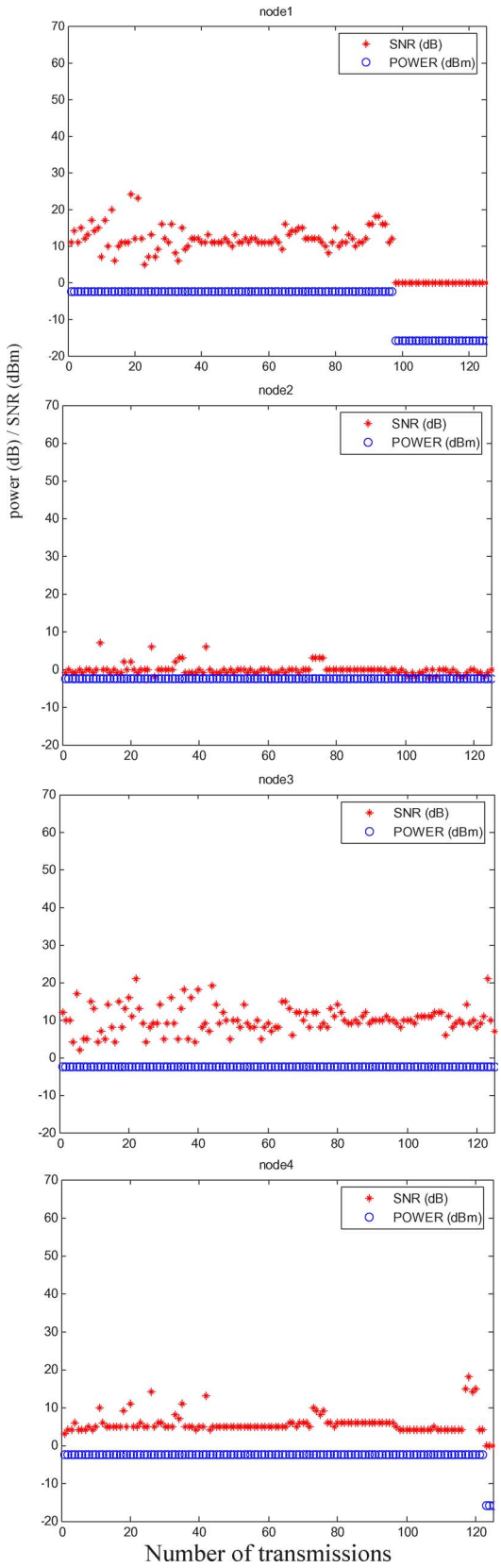

Fig. 23. RFID network performances of four nodes with no power update.

VII. Conclusion

Two algorithms for RFID reader read range and interference management based on distributed power control are explored and analyzed. Both algorithms can be implemented as power

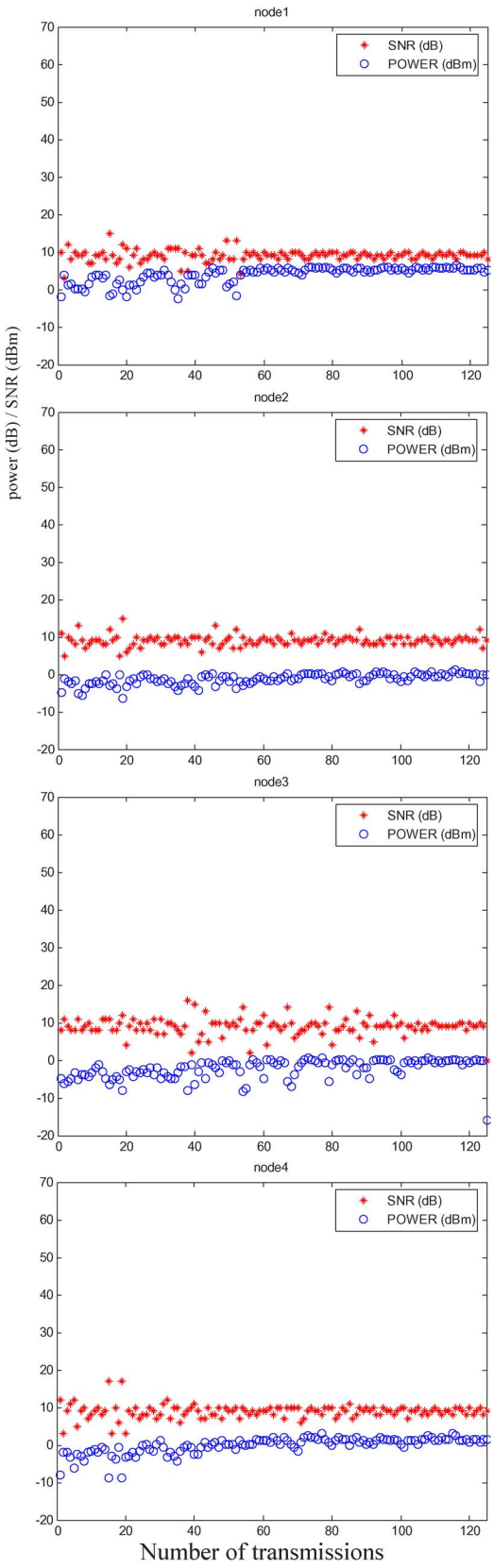

Fig. 24. RFID network performances of four nodes using DAPC.

control MAC protocols for MATLAB-based RFID reader network simulation. DAPC is seen to converge at a fast rate to the required SNR if it is achievable within power limitations. Selective back-off algorithm in DAPC enhances the channel utilization in denser networks. PPC is not fully implemented in simulation to tune in with the network density, however, it still shows advantages in scalability and fairness of channel assessment. Furthermore, the implementation details for DAPC scheme are discussed.

In this paper, we have provided a novel interpretation of the reader collision problem. We have demonstrated that high power RFID network suffers from severe interferences and causes problem on other lower power RF devices. Other distributed sensor networks, such as radar and ultrasonic systems face the similar interference problems. These problems may not be resolved easily at the RF communication level, and, therefore, a novel power control algorithm, DAPC is introduced. Finally, hardware implementation of DAPC is developed and tested for both the *ad hoc* wireless networking and RFID scenarios and shown to maintain required SNR and detection range respectively while optimizing transmission power and reducing interference levels.

REFERENCES

[1] EPCGlobal, Trenton, NJ, "EPCGlobal homepage," 2006 [Online]. Available: http://www.epcglobalinc.org/
[2] K. V. S. Rao, "An overview of back scattered radio frequency identification systems (RFID)," in *Proc. IEEE Microw. Conf.*, 1999, pp. 746–749.
[3] FCC Code of Federal Regulations, 47CFR15, Oct. 1, 2000, vol. 1, Title 47, sec. 245–249, pt. 15.
[4] D. W. Engels, "The reader collision problem," MIT Auto ID Center, Cambridge, MA, MIT-AUTOID-WH-007, 2002.
[5] U. Karthaus and M. Fischer, "Fully integrated passive UHF RFID transponder IC with 16.7-uW minimum RF input power," *IEEE J. Solid-State Circuits*, vol. 38, no. 10, pp. 1602–1608, Oct. 2003.
[6] J. Waldrop, D. W. Engels, and S. E. Sharma, "Colorwave: An anti-collision algorithm for the reader collision problem," in *Proc. IEEE ICC*, 2003, pp. 1206–1210.
[7] European Telecommunications Standards Institute, Genova, Switzerland, "TR (technical report) on LBT (listen-before-talk) for adaptive frequency agile SRD's as implemented in the Draft EN 302 288," ETSI TR 102 378 V1.1., 2005.
[8] K. Finkenzeller and R. Waddington, *RFID Handbook: Radio-Frequency Identification Fundamentals and Applications*. New York: Wiley, 2000.
[9] T. S. Rappanport, *Wireless Communications, Principles and Practices*. Englewood Cliffs, NJ: Prentice-Hall, 1999.
[10] EPC Global Hardware Action Group (HAG), "EPC radio-frequency identity protocols generation 2 identity tag (class 1): Protocol for communications at 860 MHz–960 MHz," 2003.
[11] S.-J. Park and R. Sivakumar, "Quantitative analysis of transmission power control in wireless ad-hoc networks," in *Proc. ICPPW*, 2002, pp. 1–6.
[12] E.-S. Jung and N. H. Vaidya, "A power control MAC protocol for ad hoc networks," presented at the ACM MOBICOM, Atlanta, GA, 2002.
[13] S. Jagannathan, M. Zawodniok, and Q. Shang, "Distributed power control of cellular networks in the presence of channel uncertainties," *IEEE Trans. Wireless Commun.*, vol. 5, no. 3, pp. 540–549, Mar. 2006.
[14] M. Zawodniok and S. Jagannathan, "A distributed power control MAC protocol for wireless ad hoc networks," in *Proc. IEEE WCNC*, 2004, pp. 1915–1920.
[15] K. Cha, A. Ramachandran, and S. Jagannathan, "Adaptive and probabilistic power control algorithms in dense RFID networks," in *Proc. IEEE Conf. Sens., Netw., Control*, 2006, pp. 643–648.
[16] S. Jagannathan, *Neural Network Control of Nonlinear Discrete-Time Systems*. Boca Raton, FL: Taylor and Francis, 2006.
[17] J. Fonda, M. Zawodniok, S. Jagannathan, and S. Watkins, "Development and implementation of optimal energy delay routing protocol in wireless sensor networks," in *Proc. IEEE Int. Symp. Intell. Control*, 2006, pp. 119–124.

Kainan Cha was born in Wuhan, China, on June 21, 1982. He received the M.S. degree in computer engineering from the University of Missouri-Rolla, Rolla, in 2006.

He is an Embedded Software Engineer with Garmin International, Kansas City, KS.

S. Jagannathan (SM'99) received the B.S. degree in electrical engineering from the College of Engineering, Guindy at Anna University, Madras, India, in 1987, the M.S. degree in electrical engineering from the University of Saskatchewan, Saskatoon, Canada, in 1989, and the Ph.D. degree in electrical engineering from the University of Texas, Austin, in 1994.

Since 2001, he has been with the University of Missouri-Rolla, Rolla, where he is currently a Professor and Site Director for the National Science Foundation Industry/University Cooperative Research Center on Intelligent Maintenance Systems. From 1986 to 1987, he was a Junior Engineer with Engineers India Limited, New Delhi, India. He was a Research Associate and Instructor from 1990 to 1991, at the University of Manitoba, Winnipeg, Canada. From 1994 to 1998, he worked as a consultant with the Systems and Controls Research Division, Caterpillar Inc., Peoria. From 1998 to 2001, he was with the University of Texas at San Antonio. He has coauthored more than 170 refereed conferences and juried journal articles, several book chapters, and three books entitled *Neural Network Control of Robot Manipulators and Nonlinear Systems* (Taylor & Francis, 1999), *Discrete-Time Neural Network Control of Nonlinear Discrete-Time Systems* (CRC, 2006), and *Wireless Ad Hoc and Sensor Networks: Performance, Protocols and Control* (CRC, 2007). His research interests include adaptive and neural network control, computer/communication/sensor networks, prognostics, and autonomous systems/robotics. He currently holds 17 patents and several are in process.

Dr. Jagannathan was a recipient of several gold medals and scholarships throughout his undergraduate program, the Region 5 IEEE Outstanding Branch Counselor Award in 2006, the Faculty Excellence Award in 2006, the St. Louis Outstanding Branch Counselor Award in 2005, the Teaching Excellence Award in 2005, the Caterpillar Research Excellence Award in 2001, the Presidential Award for Research Excellence from UTSA in 2001, the NSF CAREER Award in 2000, the Faculty Research Award in 2000, the Patent Award in 1996, and the Sigma Xi "Doctoral Research Award" in 1994. He has served and is currently serving on the program committees of several IEEE conferences. He is currently serving as the Associate Editor for the IEEE TRANSACTIONS ON CONTROL SYSTEMS TECHNOLOGY, IEEE TRANSACTIONS ON NEURAL NETWORKS, IEEE TRANSACTIONS ON SYSTEMS ENGINEERING, and on several program committees. He is a member of Tau Beta Pi, Eta Kappa Nu, Sigma Xi, and IEEE Committee on Intelligent Control. He is currently serving as the program chair for the 2007 IEEE International Symposium on Intelligent Control and the Publicity Chair for the 2007 International Symposium on Adaptive Dynamic Programming.

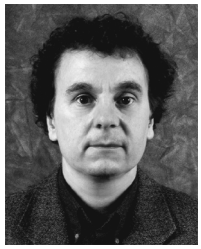

David Pommerenke received the B.S. degree in electrical engineering and the Ph.D. degree in transient fields of ESD from the Technical University Berlin, Berlin, Germany, in 1989 and 1995.

Currently, he is an Associate Professor with the Department of Electrical and Computer Engineering, University of Missouri-Rolla (UMR), Rolla. In 1989, he was a Research and Teaching Assistant in EMC and High Voltage with the Technical University Berlin. He was with Hewlett Packard for 5 years. His research interests include EMC, ESD, measurement and instrumentation.